RBSP3 (*HYA22*) is a tumor suppressor gene implicated in major epithelial malignancies

Vladimir I. Kashuba*†‡, Jingfeng Li*‡, Fuli Wang*, Vera N. Senchenko*§, Alexey Protopopov*, Alena Malyukova*¶, Alexey S. Kutsenko*, Elena Kadyrova*, Veronika I. Zabarovska*, Olga V. Muravenko*‖, Alexander V. Zelenin‖, Lev L. Kisselev‖, Igor Kuzmin††, John D. Minna‡‡, Gösta Winberg*, Ingemar Ernberg*, Eleonora Braga*¶, Michael I. Lerman**, George Klein*, and Eugene R. Zabarovsky*‖§§¶¶**

*Microbiology and Tumor Biology Center and §§Center for Genomics and Bioinformatics, Karolinska Institute, 17177 Stockholm, Sweden; †Institute of Molecular Biology and Genetics, Ukrainian Academy of Sciences, 252627 Kiev, Ukraine; §Center ''Bioengineering,'' Russian Academy of Sciences, 117312 Moscow, Russia; ¶Russian State Genetics Center, 117545 Moscow, Russia; ‖Engelhardt Institute of Molecular Biology, Russian Academy of Sciences, 119991 Moscow, Russia; **Cancer-Causing Genes Section, Laboratory of Immunobiology, Center for Cancer Research, National Cancer Institute, Frederick, MD 21702; ††Basic Research Program, SAIC-Frederick, Inc., Frederick, MD 21702; and ‡‡Hamon Center for Therapeutic Oncology Research, University of Texas Southwestern Medical Center, Dallas, TX 75390

Contributed by George Klein, February 21, 2004

Chromosome 3p21.3 region is frequently (>90%) deleted in lung and other major human carcinomas. We subdivided 3p21.3 into LUCA and AP20 subregions and discovered frequent homozygous deletions (10–18%) in both subregions. This finding strongly implies that they harbor multiple tumor suppressor genes involved in the origin and/or development of major epithelial cancers. In this study, we performed an initial analysis of *RBSP3*/*HYA22*, a candidate tumor suppressor genes located in the AP20 region. Two sequence splice variants of *RBSP3*/*HYA22* (A and B) were identified, and we provide evidence for their tumor suppressor function. By sequence analysis *RBSP3*/*HYA22* belongs to a gene family of small C-terminal domain phosphatases that may control the RNA polymerase II transcription machinery. Expression of the gene was drastically (>20-fold) decreased in 11 of 12 analyzed carcinoma cell lines and in three of eight tumor biopsies. We report missense and nonsense mutations in tumors where *RBSP3*/*HYA22* was expressed, growth suppression with regulated transgenes in culture, suppression of tumor formation in severe combined immunodeficient mice, and dephosphorylation of ppRB by RBSP3/HYA22, presumably leading to a block of the cell cycle at the G_1/S boundary.

Epithelial tumors are the most prevalent and lethal cancers and cause >80% of all cancer deaths. The short arm of chromosome 3 carries frequent and often extensive deletions in most carcinomas and some other tumor types. 3p deletions were detected in ≈100% of small cell lung (SCLC) and renal cell (RCC) carcinomas, and >80% of breast carcinomas (BC) (1–3).

On the basis of these findings, it has been postulated that human 3p contains several tumor suppressor genes (TSG) (3, 4). Some candidate TSGs have now been identified. The multistep development of the major epithelial cancers (MEC) may involve 20 or more genes from different chromosomes (5).

We have performed loss of heterozygosity analysis on >400 MECs (refs. 2 and 6 and E.R.Z., unpublished data). Two 3p21.3 regions (LUCA at the centromeric and AP20 at the telomeric borders of 3p21.3) were most frequently affected.

We have constructed detailed physical maps and sequenced these regions (7–9). For more accurate deletion mapping in MECs, we performed a combined analysis with microsatellite and *Not*I markers, comparative genome hybridization and quantitative real-time PCR (QPCR) (2, 6, 10).

We searched for homo- and hemizygous chromosome 3p losses by using 33 microsatellite markers located in frequently deleted 3p regions. Two sequence-tagged site markers NLJ-003 (AP20 region) and NL3-001(LUCA region) were used for QPCR as TaqMan probes. Frequent homozygous deletions (10–18%) were discovered in both 3p21.3 regions. More than 90% of all studied tumors showed aberrations of either NLJ-003 and/or NL3-001. It is becoming increasingly clear that these 3p21.3 subregions should be considered contiguous cancer gene regions (in analogy to contiguous gene syndromes).

The homozygous deletions affected frequently both the NLJ-003 or NL3-001 loci in the same tumor ($P < 3 \times 10^{-7}$ by permutation test) and, thus, aberrations in AP20 and LUCA regions could be causally linked. Precise analysis of 19 homozygous deletions in the AP20 region resulted in the localization of the smallest critical region to the interval flanked by D3S1298 and D3S3623 (2,6, E.R.Z., unpublished data). Only four genes were identified in this interval, namely *APRG1*, *ITGA9*, *HYA22*, and *VILL*. Here we present the analysis of one of these genes, *HYA22*.

Materials and Methods

Cell Lines and General Procedures. Cell lines were described earlier (8, 11) or were purchased from the American Type Culture Collection. Cell and tumor growth assays were as described (11, 12). All molecular biology and microbiology procedures were performed as described (13).

For RT-PCR analysis, the following 3′ UTR primers were used: *HYA22A*, 5′-GGGACACGAGGATGCCCTAA-3′; and *HYA22B*, 5′-CAGAGGCAGCCAGCCAATTT-3′.

Molecular Cloning of Human *HYA22A* and *HYA22B* Splice Variants. Gene fragments have been obtained by PCR from the Multiple Tissue cDNA (lung) panel no. K1421–1 (Clontech), using the following primer sets, according to manufacturer's manual. HYA22: 120C, 5′-GCGGCCGCCGCGCCGCGCACCCATG-GACGGCCCGGCCATC-3′ (nucleotides 351–391, see GenBank accession no. D88153 here and throughout the text if not specially mentioned); and *HYA22*C: 5′-AAAACAAAACAGGTAG-GCATGGCCACATTC-3′ (nucleotides 1,320–1,291). For sequencing internal part of the *HYA22* ORFs, the following primer was used: *HYA22D*, 5′-CTTAGCTCCTTCTTCTGCTGCTTC-CGTGATTA-3′.

5′-RACE was performed with heart Marathon ready cDNA kit according to the manufacturer's protocol with Advantage 2 PCR enzyme system (Clontech). For 5′-RACE of *HYA22*, the following primer was used: *HYA22B*, 5′-CTGACGTTGCACTGGGAG-GCTTTCTC-3′ (nucleotides 470–454).

The GenBank accession number for *RBSP3*/*HYA22A* is AJ575644 and for *RBSP3*/*HYA22B* is AJ575645. For mutational screening, AccuPrimePfx DNA polymerase and only 25–30 cycles

Abbreviations: SCLC, small cell lung carcinoma; RCC, renal cell carcinoma; BC, breast carcinoma; TSG, tumor suppressor genes; MEC, major epithelial cancers; QPCR, quantitative real-time PCR; OC, ovarian carcinoma; SCID, severe combined immunodeficient.

‡V.I.K. and J.L. contributed equally to this work.

¶¶To whom correspondence should be addressed. E-mail: eugzab@ki.se.

www.pnas.org/cgi/doi/10.1073/pnas.0401238101

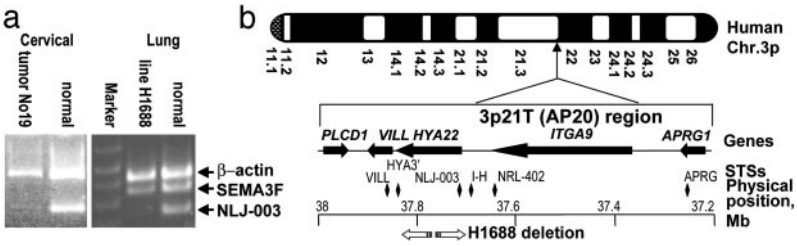

Fig. 1. Detection of homozygous deletion in AP20 region in a cervical cancer biopsy and SCLC cell line H1688 (*a*) and physical map of homozygous deletion in H1688 (*b*). Homozygous deletions were detected by using multiplex PCR. A 1-kb PLUS molecular weight marker and β-actin and SEMA3F genes in *a* are shown for comparison. *SEMA3F* has been previously found to be hemizygously deleted in the H1688. The genes in *b* are represented by pointed arrows, indicating the orientations of transcription (11).

were used (Invitrogen). This is the best performing proofreading and high-fidelity polymerase available (error rate, 2.9×10^{-6}).

DNA homology searches were performed by using BLASTX and BLASTN (14) programs at the NCBI server (www.ncbi.nlm.nih.gov/blast).

Transient Transfection and Immunostaining. To localize the corresponding proteins in cells we have prepared constructs in pCMV-TAG3a vector (Stratagene; GenBank accession no. AF072997). MCF7 breast carcinoma cell line was used in this study.

The following primary antibodies were used: rabbit against ppRB (RB phosphorylated at Ser-807/811) (Cell Signaling Technology, Beverly, MA), rabbit against RB (Sigma, R-6675), mouse monoclonal against c-myc, clone 9E10 (Oncogene Research Products). Conjugated secondary antibodies: Texas red-conjugated horse anti-mouse Ig (Vector Laboratories), FITC-conjugated swine anti-rabbit (Dako; F0205). Bisbenzimide (Hoechst 33258 from Sigma) was added at the concentration 0.4 μg/ml to the secondary antibody for DNA staining. The immunostaining was done as described (15).

QPCR. RNA was reverse transcribed by using the GeneAmp RNA PCR kit (Applied Biosystems) according to the manufacturer's protocol. The relative expression level of *HYA22* and *GAPDH* mRNAs was assessed by using QPCR (ABI PRISM 7700 Sequence Detection System, Applied Biosystems). A 129-bp fragment of *HYA22* was amplified by using MGB (3′ label nonfluorescent quencher) probe: 5′-(6-FAM)-AGAAAGCTCCCCAGTGCA-3′; forward primer, 5′-AGGTGACCAACCCCAAGGA-3′; and reverse primer, 5′-TCACGGAAGCAGCAGAAGAA-3′.

All probes and primers, including those for *GAPDH*, were purchased from Applied Biosystems. QPCR amplification was carried out in triplicate in 25-μl reaction volumes consisting of a final concentration of 1× TaqMan Universal Master Mix (Applied Biosystems), 900 nM of each primer, 250 nM *HYA22*-MGB probe, and 800 pg of cDNA.

The comparative C_T method was used as described (6).

Polymorphic and Sequence-Tagged Site (STS) Markers and Microsatellite Analysis. Physical and gene map of AP20 region, polymorphic and nonpolymorphic NLJ-003/D3S1642 markers of 3p were described earlier (6, 9). Localization of STS markers from AP20 region used in this study is shown in Fig. 1 and PCR primers were as follows: APRG: forward, 5′-AGAGAAAGCTAATAAGAAGGCAGAGAG-3′; reverse, 5′-TCGGGCGCACAATAACCTCTTTATCACA-3′; NRL402: forward, 5′-CTACTCGGGAGGCTGAGACAG-3′; reverse, 5′-CTCCTCATCCCTCATCCTGA-3′; Int-Hya: forward, 5′-TTATTCTCTGGGCTCCCCAGTT-3′; reverse, 5′-CCCAGCAAATGCTTCGTGARAA-3′; Nlj-003; forward, 5′-CAGGACTGTCTCCCACACCT-3′; reverse, 5′-GGCATGTCCAGCTCTTCTGT-3′; Hya3′: forward, 5′-GGGACACGAGGATGCCCTAA-3′; reverse, 5′-CAGAGGCAGCCAGCCAATTT-3′; VILL: forward, 5′-CTCCGACAGCATGGTCCTGA-3′; reverse, 5′-ACGGAGCTGCTGGTTCTGCT-3′; SEMA3F: forward, 5′-AGTAGGGAAGCCCAGAGAAGAA-3′; reverse, 5′-GGGGCCTATTGGTACTATCTCC-3′; ACTB: forward, 5′-GTGATGGGCCCGCTACCTCT-3′; reverse, 5′-GTAAGGCAGAGATGCACCATGTC-3′.

Results and Discussion

The Homozygous Deletion of the *HYA22* Gene in SCLC Line H1688 Is Intragenic. We have found (2, 6) that the NLJ-003 locus was homozygously deleted in ≈15% of the MEC. Deletions in SCLC cell line H1688 and cervical carcinoma biopsy are shown as examples (Fig. 1*a*). We mapped the H1688 deletion precisely by using additional polymorphic and nonpolymorphic markers (Fig. 1*b*). Markers located between 3′ end of *ITGA9* and 5′ end of *HYA22* (Int-HYA or I-H) and in the 3′ end of the *HYA22* (HYA3′) gave positive signals with H1688 DNA. Both breakpoints are inside the *HYA22* gene and do not affect exons of either *ITGA9* or *VILL* genes.

Identification of Two Splice Variants: *HYA22A* and *HYA22B*. A set of overlapping human cDNA sequences was obtained through a combination of cDNA library screening and RACE-PCR. Analysis of all obtained sequences revealed three main features. First, these sequences could not reach the predicted 5′ end of the *HYA22* (GenBank accession no. D88153) (16), confirming that all human EST clones in public databases end at position 351 nt.

Second, we have found that the *HYA22* sequence established in our experiments differs from what was published previously by deletion of a G nucleotide at position 187 of D88153, and is in agreement with the genome draft sequence (GenBank accession nos. AC093415 and AP006242). That means that the ATG codon suggested by Ishikawa *et al.* (16) cannot work as an initiating codon for the postulated ORF. We suggest another initiating codon in our cDNA sequence, corresponding to ATG at nucleotide position 373 of *HYA22* sequence (GenBank accession no. D88153). Further comparisons between our genomic sequence and that of Ishikawa *et al.* (16) revealed another error: the TC dinucleotide (127–128 position in the predicted sequence; ref. 16) has not been detected in the genomic sequence. In this position, suggested previously as a border between exons 1 and 2, we could not find any sign of splicing signals. We therefore think that the first exon and the initiating codon may have been incorrectly identified. Alignment with *HYA22* genes from other species is consistent with our conclusion because the similarity starts just at the second Met codon in D88153 (Fig. 2). There is a similar situation in the mouse genome with the previously identified by us *MYA22* gene (GenBank accession no. AJ344340). We have shown that the first ATG in *MYA22* cannot serve as initiating codon because careful analysis of cDNA and genomic sequences revealed that it is not in frame with the second ATG.

Third, we have isolated two *HYA22* splicing variants termed *HYA22A* (accession No. AJ575644) and *HYA22B* (GenBank accession no. AJ575645). The major difference between them is that HYA22A protein lacks 11 amino acids (79–89 amino acids in HYA22B, nucleotides 257–289 in AJ575645). Importantly, similar A and B forms have been identified in the chicken *HYA22* gene (*NIF1T1* and *NIF1R5*, GenBank accession nos. AF189776 and AF189773; see Fig. 2).

Overall, *HYA22* has highly conserved orthologs (and paralogs) in

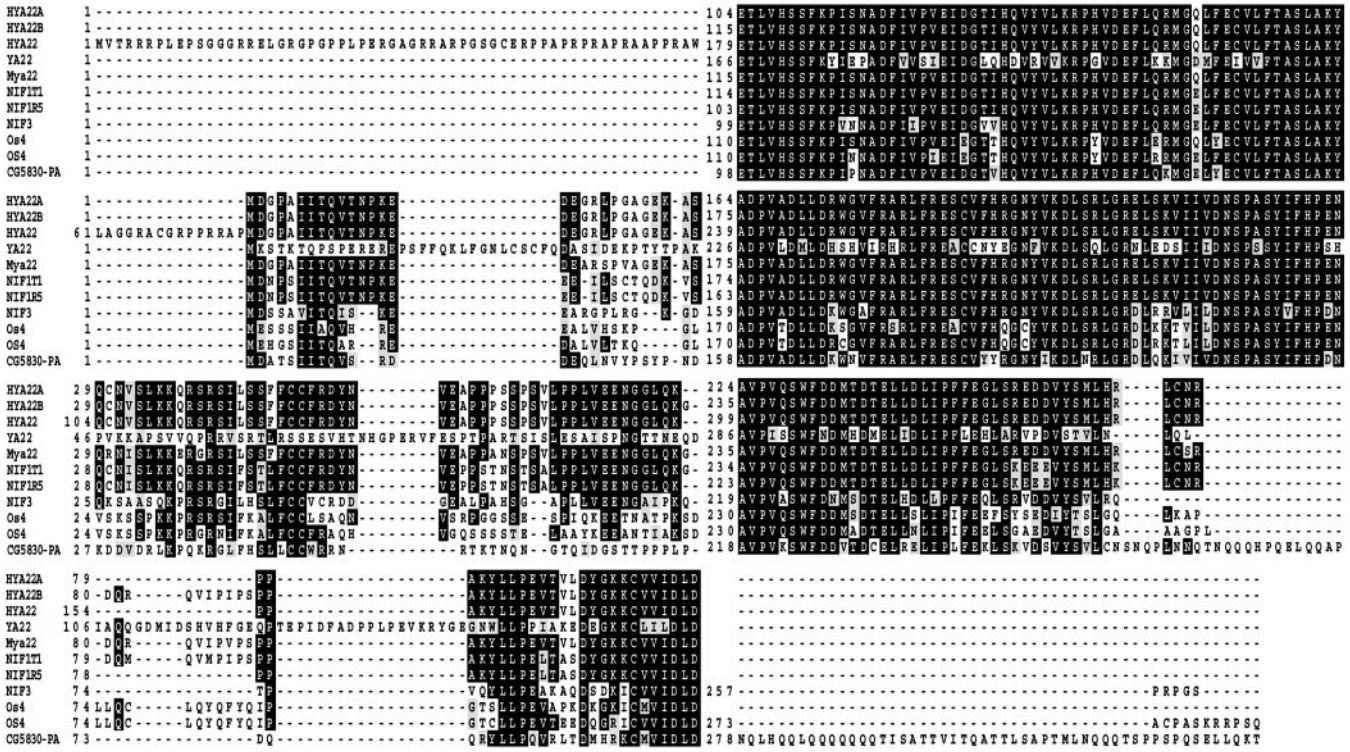

Fig. 2. Alignment of the predicted amino acid sequences of the family of *SCP*/*HYA22* related genes (not all members are shown). Amino acid sequences used for the alignment were as follows: HYA22A (CAE11804), HYA22B (CAE11805), HYA22 (BAA21667) *Homo sapiens* YA22 like protein, yeast hypothetical YA22 protein (Q09695), Mya22 (CAC69078) NIF-like protein (*Mus musculus*), NIF1T1 (AAF17481) NLI-interacting factor isoform T1 (*Gallus gallus*), NIF1R5 (AAF17484) NLI-interacting factor isoform R5 (*G. gallus*), NIF3 (Q9GZU7) nuclear LIM interactor-interacting factor 3 (NLI-interacting factor 3) (*H. sapiens*), Os4 (AAL34532) (*Xenopus laevis*), OS-4 (AAB71816) (*H. sapiens*), CG5830-PA (AAF49553) (*Drosophila melanogaster*). *HYA22A* is identical to *SCP3* (small CTD phosphatase 3), *NIF3* to *SCP1* and *OS-4* to *SCP2* (21). It is clear that 5′ amino acid HYA22 sequence predicted in BAA21667/D88153 is not similar to any other members.

many species (Fig. 2). The yeast ortholog, YA22, shows ≈70% identity over the most conserved region, whereas the rodent, chicken, and human proteins are almost identical. HYA22 shows strong similarity with several other proteins, e.g., from *Caenorhabditis elegans*, *Arabidopsis thaliana*, *Schizosaccharomyces pombe*, *Dictyostelium discoideum*, and rice *Oryza sativa* (data not shown).

Methylation Status of the 5′ Region of *HYA22*. We have recently reported that the AP20 (3p21.3T) region is heavily methylated in RCC cell lines and biopsies (9). However, direct bisulphite sequencing of six RCC cell lines in the area between 9,654 and 10,088 (5′ end CpG island) nucleotides (positions from the draft genome sequence, GenBank accession no. AP006242) did not reveal any methylation. Probably, we still failed to identify the correct CpG island associated with *HYA22* promoter activity.

Preliminary Expression and Mutational Analysis of *HYA22*. We have performed RT-PCR expression analysis on 14 prostate and 8 cervical biopsies, 13 lung and 12 RCC cancer cell lines and, with the exception of one prostate sample, we could observe some PCR bands. In this case, primers to 3′ UTR *HYA22* were used (see *Materials and Methods*). We have also performed QPCR analysis of *HYA22* expression in 12 MEC cell lines, four RCC, two BC, and two ovarian carcinoma (OC) biopsies (Fig. 3*a*). Here, primers were designed on the border between second and third exons, i.e., at the 5′ end. In 11 of 12 cell lines, we have detected a significant decrease of expression (the ACC-LC5 cell line with homozygously deleted *HYA22* was used as a negative control, in 10 others it was <5%). In one line, SCLC N417, a 39-fold increase of expression was seen. A similar pattern was found in tumor biopsies: in only three (two RCC and one BC) of eight biopsies, there was a significant decrease of expression (>2-fold: T3, T4, and T8, Fig. 3*a*). In two of them, expression increased more than two times (one RCC, T2, and one OC, T6). We detected 8-fold amplification of the genomic copy number in NLJ-003 in the RCC case with increased expression (T2).

HYA22 was sequenced in both T2 and T6 biopsies with increased expression, and mutations were detected in both cases. In the OC T6 biopsy exons 2 and 3 were deleted, and a premature stop codon appeared in exon 4. In the RCC T2 biopsy, a missense mutation Ser121Pro was discovered.

We have also sequenced three other cancer biopsies with the expressed *HYA22* and found missense mutations: in RCC T1, it was Asn127Ser; and in OC T5 and BC T7, it was Val132Gly. Sequencing of *HYA22* in the N417 cell line revealed mutation His139Tyr.

RT-PCR is too sensitive and can detect *HYA22* transcripts from contaminating normal cells. It is also known (9) that two other highly related paralogous genes (*OS-4* and *NIF3*) are present in the human genome (see Fig. 2). Moreover, BLAST search revealed in the human genome numerous nearly identical short sequences that could increase the background and may lead to incorrect results. Northern analysis of 17 RCC cell lines revealed weak expression in 12 RCC lines (for example, see Fig. 3 *b* and *c*). More studies are needed to understand the aberrant nature of *HYA22* expression in tumors. Our preliminary analysis did not discriminate between *HYA22A* and *HYA22B*, which could be very important [for example, see Dammann *et al.* (17) for *RASSF1A* and *RASSF1C* forms]. However, these initial studies revealed that the changes have a complex character, and at least seven mutations were found (including the intragenic deletion in H1688). We tested these mutations in all publicly available sequenced *HYA22* clone isolates from normal cells and did not find any of our mutations. Thus, they most

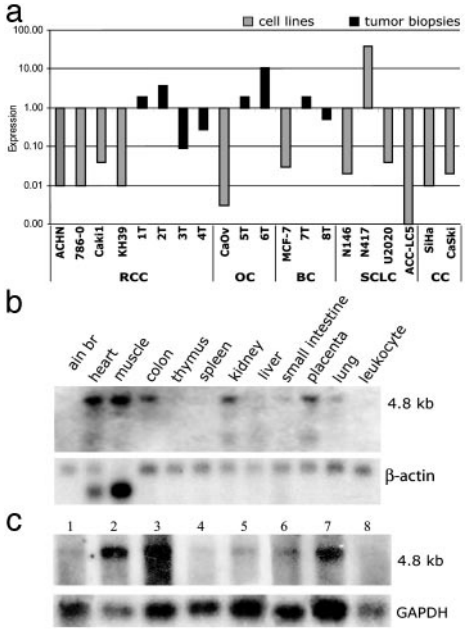

Fig. 3. Expression analysis of *HYA22* in cancer and normal cells. (*a*) QPCR mRNA expression profile of *HYA22* for different cancer cell lines and tumor biopsies compared to normal tissues. The *y* axis indicates the value of the samples that are shown in $\log_{10}$ scale relative to control normal tissues normalized to 1.0. The *x* axis shows the samples. (*b*) Northern analysis of *HYA22* expression (4.8 kb mRNA) in normal tissues by using human multiple tissue Northern blot (Clontech, no. 7765-1). (*c*) Northern analysis of *HYA22* expression (4.8 kb mRNA) in cancer cell lines. Two micrograms of poly(A+) mRNA from RCC cell lines 786–0 (lane 1), UOK206 (lane 2), UOK143 (lane 3), UOK127 (lane 4), UOK121 (lane 5), UOK102 (lane 6), RFX393 (lane 8), and SCLC line COR-L24 (lane 7) were loaded per lane. CC, ovarian carcinoma.

likely are not polymorphisms. Seven more mutations were found in severe combined immunodeficient (SCID) mouse experiments (see below).

Growth-Inhibiting Activity of *HYA22A* and *HYA22B in Vitro* and *in Vivo*. To test the ability of *HYA22* to suppress tumor growth *in vitro*, we performed colony formation assays using KRC/Y cells and selecting for the *Bsd* gene carried by pETE vector. The pETE vector without insert was used as a negative control. Fig. 4 shows that both *HYA22* isoforms inhibited colony formation.

Both *HYA22A* and *HYA22B* forms were entered into gene inactivation test (GIT) as described by Li *et al.* (18) and Protopopov *et al.* (11). This test is based on the functional inactivation of the analyzed genes. Our hypothesis was that TSG must be inactivated in growing tumors under experimental conditions. This can be achieved in different ways: deletion, mutation, methylation, etc.

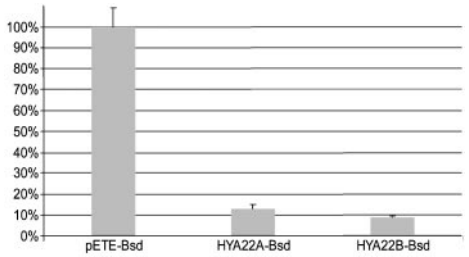

Fig. 4. The effect of expression *HYA22A* and *HYA22B* genes on colony formation of KRC/Y cells. Efficiency of colony formation for the pETE vector is taken as 100% (*y* axis).

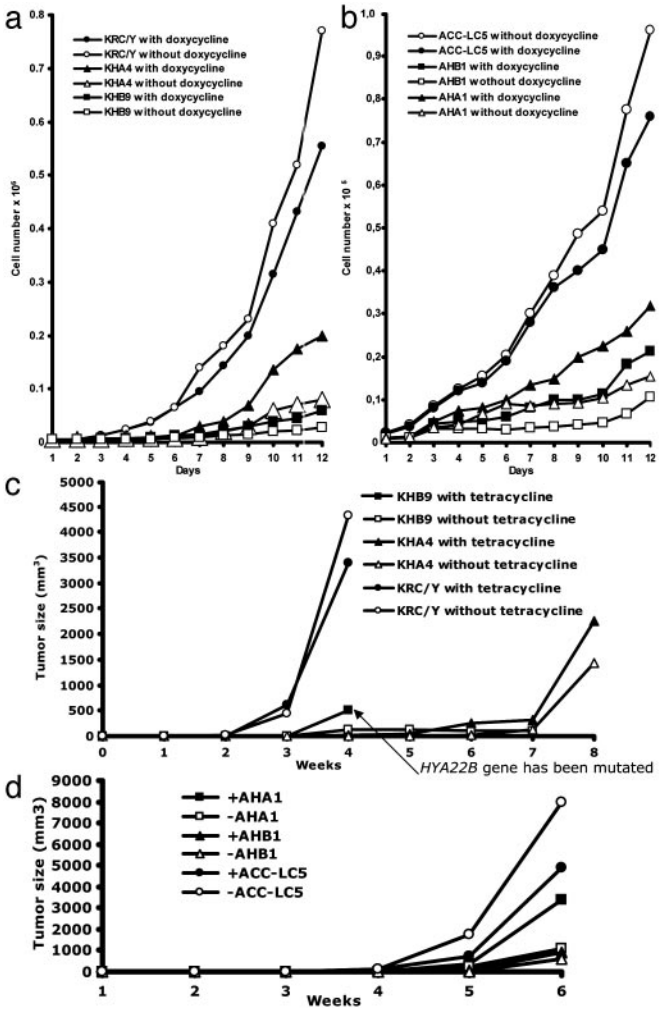

Fig. 5. Growth suppression with *HYA22 in vitro* and *in vivo*. Growth inhibition of KRC/Y (*a*) and ACC-LC5 (*b*) cells by *HYA22A* (clones KHA4 and AHA1) and *HYA22B* (KHB9 and AHB1) genes *in vitro* are shown, as are tumor growth inhibition of KRC/Y (*c*) and ACC-LC5 (*d*) cells by *HYA22A* and *HYA22B in vivo*.

Both forms have been cloned into episomal tetracycline-regulated pETE vector, and their sequences were confirmed. pETE-A containing *HYA22A* and pETE-B with *HYA22B* were transfected into cells that produced tetracycline transactivator tTA constitutively. Two cell lines were used: the RCC line KRC/Y (K712), where expression of the gene was hardly detectable by Northern hybridization, and the SCLC line ACC-LC5, where the gene was homozygously deleted. Four clones that showed the best tetracycline regulation have been selected: the KRC/Y clones *HYA22A*-cl.4 (KHA4) and *HYA22B*-cl.9 (KHB9) and, in ACC-LC5 clones, *HYA22A*-LC5cl.1 (AHA1) and *HYA22B*-LC5cl.1 (AHB1).

All clones were tested for growth on plastic Petri dishes in the absence or presence of doxycycline. They were monitored daily by counting cells from triplicate dishes. The original cells with the empty vector and/or original cells were used as a control (both produced the same results). Fig. 5 *a* and *b* shows the results. Both *HYA22A* and *HYA22B* suppressed cell growth in the absence of doxycycline (72–93% suppression on day 7 and 84–96% suppression on day 12). Even in the presence of doxycycline, there was a clear growth inhibition effect. This could be explained by at least two factors. Even weak expression of the *HYA22* due to the leakage could have a strong growth-inhibiting effect. Doxycycline itself has some inhibiting effect, however. In experiments with KRC/Y and

Table 1. Summary of gene inactivation test using *HYA22* genes and ACC-LC5 and KRC/Y cells

Genes	Clone	Tetracycline	Tumors	PCR	Northern	Mutation
KHB	Clone 9	−	T1	−	−	
		+	T2	+	Very weak	L192P
		−	No			
		+	No			
		−	No			
		+	No			
KHA	Clone 4	−	T3	Weak	Weak	I7L,F111L
		+	T4	+	−	
		−	No			
		+	T5	+	−	
		−	No			
		+	No			
AHB	Clone 1	−	T6	−		
		+	T7	−		
		−	T8	Weak	Weak	L192P
		+	T9	+	Very weak	C30R,Q77R
		−	T10	−		
		+	T11	−		
AHA	Clone 1	−	T12	Weak	Weak	M1K
		+	T13	+	Weak	delG (nt 35)*
		−	T14	−		
		+	T15	−		
		−	T16	−		
		+	T17	Weak	Weak	delT (nt 150)*

*GenBank accession no. AJ575644.

ACC-LC5 concentration, 200–500 ng of doxycycline induced 15–25% growth retardation, similarly to published observations (19). In contrast to the original cell lines, the cells carrying *HYA22A* and *HYA22B* were growing 2.5–3 times faster in the presence of doxycycline.

The clones were inoculated into six SCID mice (5×10^6 cells per mouse). Three were given drinking water containing 1 mg/ml tetracycline, whereas the other three were given drinking water without tetracycline. Nontransfected KRC/Y and ACC-LC5 cells were used as controls. Results are shown in Fig. 5 *c* and *d*. Seven of 24 inoculations of *HYA22* transfected cells did not grow at all. All other cases showed strong inhibition of tumor growth compared to controls. There was a 1.5- to 2-fold difference in tumor growth between mice drinking water with and without tetracycline. It is known that tetracycline is a weaker inhibitor of expression than doxycycline in the tTA system, and it is likely that leakage is stronger *in vivo* in SCID mice than *in vitro*.

After 6–9 weeks, the remaining 17 tumors were explanted and tested for the presence of the pETE-A and pETE-B constructs by PCR (see Table 1 and Fig. 6*a*). The introduced *HYA22* genes were detected in five tumors, and in four they were detected but at very low level. All these nine cases where *HYA22* genes have been detected were further examined with Northern hybridization. Weak hybridization was detected in five tumors, hardly detectable in two (T2 and T9), and undetectable in T4 and T5 (Fig. 6*b*). Seven tumors expressing *HYA22* were sequenced to check for possible mutations, and in all cases mutations were found. In two cases, it was deletion of one nucleotide (T13, T17) and in one case the initiating codon was destroyed (T12). The summary of the GIT assay is presented in Table 1. Importantly, no mutations were found in *HYA22* in KRC/Y cells growing *in vitro*.

In conclusion, the *HYA22* genes were inactivated in all xenografts showing growth by either deletion, loss of expression, or mutations. We have obtained similar results in previous experiments where the human *RB1* gene was transfected and expressed in the mouse A9 fibrosarcoma cell line under the tetracycline regulation. After

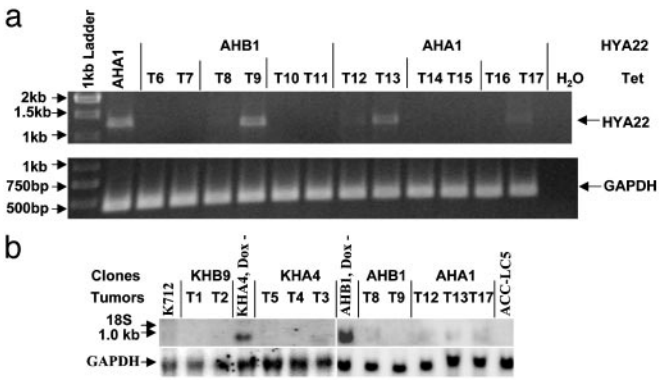

Fig. 6. Analysis of SCID tumors for the presence of transduced *HYA22* genes by PCR (*a*) and their expression by Northern hybridization (*b*).

passage of the *RB1* transfectants through SCID mice, the wild-type *RB1* gene was deleted or functionally inactivated already after the first passage in all 20 tumors tested (18).

It is worthwhile to mention that both *HYA22* forms had a strong growth inhibiting effect even in the presence of doxycycline or tetracycline. *HYA22* is normally expressed in lung and kidney tissue (see Fig. 3*b*, ref. 16; see GeneNote: Human Gene Normal Tissue Expression at http://genecards.weizmann.ac.il), and leaking expression is hardly detectable in the selected *HYA22* transfected clones. This means that the suppressor activity is not dependent on abnormally high ectopic transgene expression and constitutes intrinsic feature of the gene function.

Possible Mechanisms of *HYA22* Action in Tumorigenesis: Dephosphorylation of RB by Transient Expression of HYA22 Isoforms. Preliminary analysis of expression of *HYA22* revealed that changes in MEC biopsies and cell lines could be completely opposite: both elevated and decreased expression compared to normal cells was observed

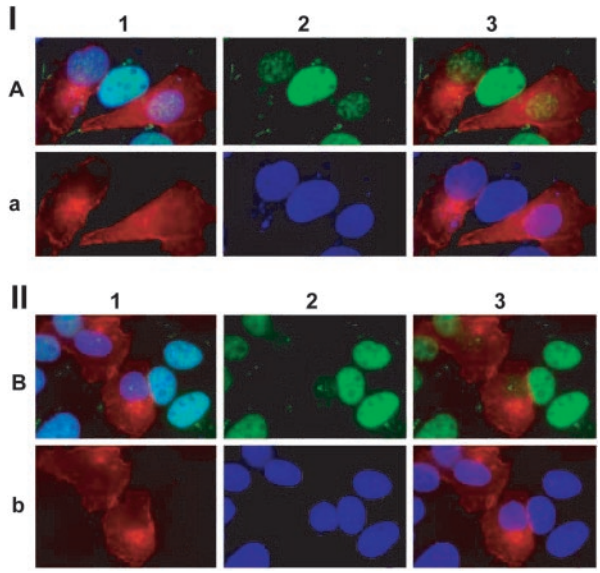

Fig. 7. Effect of the *HYA22A* (*I*) and *HYA22B* (*II*) genes on the presence of phosphorylated RB. MCF7 cells, transfected with *HYA22A* and *HYA22B* containing c-myc tag, were analyzed with immunofluorescence microscopy. c-myc tag was labeled with red, phosphorylated RB was labeled with green, and DNA was labeled with blue. A1 and B1, superimposition of all three colors; A2 and B2, green only; A3 and B3, superimposition of green and red; a1 and b1, red only; a2 and b2, blue only; a3 and b3, superimposition of red and blue. MCF-7 cells express endogenous HYA22 at a very low level (see Fig. 3).

(Fig. 3). In three of eight biopsies, there was a significant decrease of expression, and expression increased in two biopsies. A similar pattern was found in MEC cell lines.

This finding is reminiscent of the loss of heterozygosity and QPCR studies: *HYA22* was deleted in 48–74% of MECs and amplified in 17–34% (ref. 6 and E.R.Z., unpublished data).

In one RCC biopsy with increased expression, we detected 8-fold amplification of the genomic copy number in NLJ-003 (DNA from another biopsy, OC, was not available). Moreover, 14 *HYA22A* mutations (including four nonsense and one destroying initiating Met codon) were detected in RCC, OC, BC, and SCLC biopsies/cell lines and in experimental SCID tumors expressing *HYA22*.

Interestingly, this gene was deleted during the construction of the original cosmid contig covering the ACC-LC5 deletion, suggesting its poison effect, and yeast cells that lack *YA22* lose viability (16). Furthermore, the closely related *OS-4* is most likely involved in the development of human sarcomas (20).

The *HYA22* gene product contains the nuclear LIM interactor (NLI)-interacting domain. It is possible that *HYA22* may function as coordinator of transcriptional activity via its interaction with NLI.

During the preparation of this manuscript, Yeo *et al.* (21) published a paper showing that *HYA22A* (they called the gene *SCP3*) is a member of a previously uncharacterized family of small C-terminal domain (CTD) phosphatases, *SCP*. Two other members are *SCP1* (previously *NIF3*) and *SCP2* (also called *OS-4*). They demonstrated phosphatase activity for SCP1 and SCP2 and suggested that all of these proteins catalyze the dephosphorylation of Ser 5 within the consensus repeat of the largest RNA polymerase II subunit (RNAPII) and affect gene transcription. They did not exclude the possibility that *SCPs* influence the phosphorylation state of other substrates than CTD. Our previous results and this study suggest that one of the functions of *SCP3/HYA22* can be very important for the development of MEC.

In our experiments, we observed that *HYA22A* has lower inhibition activity than *HYA22B*. Thus, it is likely that these two isoforms possess both similar and different functions and the balance between A and B forms may be crucial for the process of carcinogenesis. It is therefore important during mutation screening to check for mutations that could influence splicing patterns. Clearly, the interaction with other *SCPs* also is very important.

To analyze for a possible tumor suppressor function of *HYA22* as a phosphatase regulating the cell cycle, we explored whether it could influence the phosphorylation status of pRB and thereby positively regulate its function.

Both HYA22A– and HYA22B–mycTAG fusion proteins were expressed mainly in the cytoplasm of transiently transfected cells (Fig. 7). The accumulation in the intracellular membrane components was also seen in the transfected cells. The level of phosphorylated RB (we used antibodies specific for RB protein phosphorylated at Ser-807 and Ser-811) in the transfected cells was significantly decreased, especially when *HYA22* form B was expressed. However, when antibody to the total Rb was used, the amount of RB protein was approximately the same in all cells (data not shown). This experiment again suggested that HYA22 proteins could work as phosphatases involved in the regulation of cell growth and differentiation. It was previously suggested that, in contrast to oncogenes with kinase function, phosphatases with TSG activity should exist. Because *HYA22* was a temporary name, we suggest to rename the gene *RBSP3*, i.e., RB1 serine phosphatase from human chromosome 3.

Interestingly, that both *RASSF1* (TSG from the LUCA region) and *RBSP3* could help each other in induction of cell cycle arrest: the former by inhibiting cyclin D1 (22) and the latter by activating RB protein. This could explain frequent homozygous deletions both in LUCA and in AP20 regions in the same tumor and support the hypothesis that TSGs in these two regions could have a synergistic effect (see Introduction).

Finally, we have shown that the *RBSP3* gene is located at the chromosome region that is very frequently hemizygously and homozygously deleted in various malignancies. The gene is expressed at a very low level compared with normal cells in several MEC. We have also found mutations in the *RBSP3* in natural and experimental tumors where it is expressed. Preliminary analysis of EST databases also revealed the occurrence of nonsense mutations in RBSP3/HYA22 clones obtained from tumor cells/tissues (e.g., BF002474, BG111423). *In vitro* and *in vivo* experiments demonstrated cell and tumor growth-inhibiting activity. Its transient expression resulted in drastic reduction of phosphorylated form of RB1 protein and thus probably blocking the cell cycle at the G_1/S boundary. The *RBSP3* gene is highly conserved from yeast to human.

All of these features are consistent with the classical characteristics of a TSG. However, because of possible amplification of its mutated forms and possible ability to act in a dominant-negative fashion, *RBSP3* could also represent a previously undescribed class of cancer-causing genes with both tumor suppressor and oncogenic activity.

We are grateful to Drs. D. Uzhametsky and E. Kashuba for assistance in some experiments. This work was supported by research grants from the Swedish Cancer Society, the Swedish Research Council, the Swedish Foundation for International Cooperation in Research and Higher Education (STINT), the International Association for the Promotion of Cooperation with Scientists from the New Independent States of the Former Soviet Union (INTAS), the Children Cancer Foundation, the Swedish Institute, the Royal Swedish Academy of Sciences, and Karolinska Institute. O.V.M., A.V.Z., E.B., and L.L.K. were supported by the Russian National Human Genome Program and Russian Foundation for Basic Research Grant 01-04-48028. I.K. and M.I.L. were funded *in toto* with funds from the National Cancer Institute, National Institutes of Health, under Contract NO1-CO-56000. J.D.M. was supported by Lung Cancer Specialized Programs of Research Excellence P50 CA70907 and CA71618.

1. Wistuba, I. I., Gazdar, A. F. & Minna, J. D. (2001) *Semin. Oncol.* **28,** 3–13.
2. Imreh, S., Klein, G. & Zabarovsky, E. R. (2003) *Genes Chromosomes Cancer* **38,** 307–321.
3. Zabarovsky, E. R., Lerman, M. I. & Minna, J. D. (2002) *Oncogene* **21,** 6915–6935.
4. Kok, K. Naylor, S. L. & Buys, C. H. (1997) *Adv. Cancer Res.* **71,** 27–92.
5. Zochbauer-Muller, S., Gazdar, A. F. & Minna, J. D. (2002) *Annu. Rev. Physiol.* **64,** 681–708.
6. Senchenko, V., Liu, J., Braga, E., Mazurenko, N., Loginov, W., Seryogin, Y., Bazov, I., Protopopov, A., Kisseljov, F. L., Kashuba, V., *et al.* (2003) *Oncogene* **22,** 2984–2992.
7. Wei, M. H., Latif, F., Bader, S., Kashuba, V., Chen, J. Y., Duh, F. M., Sekido, Y., Lee, C. C., Geil, L., Kuzmin, I., *et al.* (1996) *Cancer Res.* **56,** 1487–1492.
8. Lerman, M. I., Minna, J. D., Sekido, Y., Bader, S., Burbee, D., Fong, K., Forgacs, E., Gao, B., Garner, H., Gazdar, A. F., *et al.* (2000) *Cancer Res.* **60,** 6116–6133.
9. Protopopov, A., Kashuba, V., Zabarovska, V. I., Muravenko, O. V., Lerman, M. I., Klein, G. & Zabarovsky, E. R. (2003) *Cancer Res.* **63,** 404–412.
10. Li, J., Protopopov, A., Wang, F., Senchenko, V., Petushkov, V., Vorontsova, O., Petrenko, L., Zabarovska, V., Muravenko, O., Braga, E., *et al.* (2002) *Proc. Natl. Acad. Sci. USA* **99,** 10724-10729.
11. Protopopov, A. I., Li, J., Winberg, G., Gizatullin, R. Z., Kashuba, V. I., Klein, G. & Zabarovsky, E. R. (2002) *J. Gene Med.* **4,** 397–406.
12. Dreijerink, K., Braga, E., Kuzmin, I., Geil, L., Duh, F. M., Angeloni, D., Zbar, B., Lerman, M. I., Stanbridge, E. J., Minna, J. D., *et al.* (2001) *Proc. Natl. Acad. Sci. USA* **98,** 7504–7509.
13. Zabarovsky, E. R., Kashuba, V. I., Zakharyev, V. M., Petrov, N., Pettersson, B., Lebedeva, T., Gizatullin, R., Pokrovskaya, E. S., Bannikov, V. M., Zabarovska, V. I., *et al.* (1994) *Genomics* **21,** 495–500.
14. Gish, W. & States, D. J. (1993) *Nat. Genet.* **3,** 266–272.
15. Pokrovskaja, K., Mattsson, K., Kashuba, E., Klein, G. & Szekely, L. (2001) *J. Gen. Virol.* **82,** 345–358.
16. Ishikawa, S., Kai, M., Tamari, M., Takei, Y., Takeuchi, K., Bandou, H., Yamane, Y., Ogawa, M. & Nakamura, Y. (1997) *DNA Res.* **4,** 35-43.
17. Dammann, R., Li, C., Yoon, J. H., Chin, P. L., Bates, S. & Pfeifer, G. P. (2000) *Nat. Genet.* **25,** 315–319.
18. Li, J., Protopopov, A. I., Gizatullin, R. Z., Kiss, C., Kashuba, V. I., Winberg, G., Klein, G. & Zabarovsky, E. R. (1999) *FEBS Lett.* **451,** 289-294.
19. Rubins, J. B., Charboneau, D., Alter, M. D., Bitterman, P. B. & Kratzke, R. A. (2001) *J. Lab. Clin. Med.* **138,** 101–106.
20. Su, Y. A., Hutter, C. M., Trent, J. M. & Meltzer, P. S. (1996) *Mol. Carcinog.* **15,** 270–275.
21. Yeo, M., Lin, P. S., Dahmus, M. E. & Gill, G. N. (2003) *J. Biol. Chem.* **278,** 26078–26085.
22. Shivakumar, L., Minna, J., Sakamaki, T., Pestell, R. & White, M. A. (2002) *Mol. Cell. Biol.* **22,** 4309–4318.